Published in International Journal of Energy Research with doi: 10.1002/er.8058

A Novel Interval-based Formulation for Optimal Scheduling of Microgrids with Pumped-Hydro and Battery Energy Storage under Uncertainty

Saeid Ahmadi[1], Marcos Tostado-Véliz[2], Ali Asghar Ghadimi[1], Mohammad Reza Miveh[3], and Francisco Jurado[1,*]

1. *Department of Electrical Engineering, Faculty of Engineering, Arak University, Arak 38156-8-8349, Iran (e-mail: sa.ahmadi1995@gmail.com (S.A.) and a-ghadimi@araku.ac.ir (A.A.G.)).*
2. *Department of Electrical Engineering, University of Jaén, 23700 EPS Linares, Jaén, Spain (e-mail: mtostado@ujaen.es (M.T.-V.) and fjurado@ujaen.es (F.J.)).*
3. *Department of Electrical Engineering, Tafresh University, Tafresh 39518-79611, Iran (e-mail: miveh@tafreshu.ac.ir).*

* *Correspondence: fjurado@ujaen.es*

Abstract - Nowadays, microgrids are emerging as an invaluable framework for the integration of renewable energy sources and demand response programs. In such systems, energy storage facilities are also frequently deployed to properly manage surplus energy from renewable sources on pursuing more efficient management of the system. Hybrid storage systems in which various storage facilities are combined may result in a more effective solution than only considering one storage technology. This way, the good features of the different technologies may be jointly exploited while their drawbacks are minimized. Due to the large-scale integration of renewable energies in this kind of grid, coping with uncertainties becomes a critical issue. Moreover, the operation of microgrids frequently deals with other kinds of uncertainties related to energy pricing from the upscale grid (in the case of grid-connected mode) or local demand. This way, proper modelling of uncertainties is essential for adequately operating these systems. This paper contributes to this pool by developing a novel interval-based formulation, for optimal scheduling of microgrids considering battery and pumped-hydro storage systems. To achieve this goal, the optimal scheduling of a microgrid with pumped-hydro and battery energy storage considering demand response is modeled, firstly. Then, the new interval-based formulation is used to cope with the uncertainties. Finally, the suggested model is verified using simulations in various cases, and the results confirm the effectiveness of the novel interval-based formulation for the optimal scheduling of microgrid with pumped-hydro and battery energy storage under uncertainty.

Keywords - Microgrid, uncertainty, robust optimization, interval optimization, renewable energy, pumped-hydro storage, battery energy storage

Nomenclature

Indexes (Sets)

$t(\mathcal{T})$	Time
$j(J)$	Price level
$n(N)$	Deterministic constraint
$k(K)$	Interval-based inequalities
$m(M)$	Interval-based equalities

Superscripts

$\mathrm{G}, \mathrm{buy/sell}$	Upscale grid in buying and selling mode
PBDR	Price-based demand response
PV	Photovoltaic panels
$\mathrm{B}, \mathrm{ch/dch}$	Batteries in charging/discharging mode
PHS, p/t	Pumped hydro storage in pump/turbine mode
Upper/Lower	Upper/lower water reservoir
$\overline{(\cdot)}, \underline{(\cdot)}$	Maximum/minimum value
LB, UB	Lower bound/Upper bound for interval model

Parameters

$\Delta\tau$	Time step [h]
π	Energy Price [$/kWh]
g	Gravity acceleration [m/s²]
H	Net head [m]
ρ	Water density [kg/m³]
η	Efficiency [pu]
μ	Operation and maintenance cost [$/kWh or $/kWh²]
σ	Start-up and shutdown costs [$]
R	Ramp rate limit [kW]
D	MG demand [kW]
e2P	Energy to power ratio [h]
L	Demand response rate
λ	Probability degree [pu]

J	Price rate
ϑ	Solar irradiation [kW/m²]
θ	Temperature [ºC]
Decision variables (x)	
p	Power [kW]
ε	Energy [kWh]
q	Water flow [m³/s]
u	Commitment status [Binary]
on/off	On/off status of assets [Binary]
v	Water volume [m³]

1 - Introduction

1.1 - Background

Nowadays, public entities are encouraging the use of renewable energy sources (RESs) such as photovoltaic (PV) and wind-based generators, with the aim of decarbonizing the electricity sector and thus reducing to the minimum the use of fossil fuels and greenhouse gas emissions [1]. As a representative example, European Union agreed upon a 20% RES target for 2020 [2] and 32% by 2030, with a review for increasing this figure in 2023 [3]. The intermittent and non-dispatchable nature of RESs will make essential the widespread use of energy storage to meet such an ambitious goal. Battery systems are currently one of the most used and investigated technologies for electricity storage [4]. This technology enables a high-efficient chain for energy storage through electro-chemical reactions. However, high-energy density technologies are not mature yet and depositions of some metals like lithium may be environmentally harmful [5]. To circumvent the limitations of battery energy storage (BES) facilities, different storage technologies may be combined in order to jointly exploit the advantages of each one [6]. In this regard, pumped-hydro storage (PHS) units, although less efficient, are able to provide large-scale storage capacity, being so an ideal complement to batteries, enabling a more efficient management of renewable sources [7].

To further integrate energy storage technologies with other initiatives and agents like demand response (DR) programs and charging infrastructures [8], microgrids (MGs) have emerged as a valuable solution [9]. This kind of system can be defined as small-scale grids with the capability of being operated in both grid-connected and isolated modes [10]. Flexible operation of such networks is enabled via bidirectional communication channels among consumers, generation units and the MG operator, being possible to exchange information among them. Taking advantage of this wide communication among agents, energy management systems (EMSs) are used to properly coordinate the operation of the different devices and consumers. This kind of program performs the day-ahead or real-time scheduling of the different assets on pursuing economic or environmental goals. Conventionally, EMSs must work under stochastic environments due to the unpredictable behaviour of RESs and consumers. This paper is focused on this issue.

1.2 - Literature review

In recent years, uncertainties modelling in MGs has attracted huge attention in multiple research items. Ref. [11] proposed a scenario-based optimization framework for reactive power scheduling in a grid-connected MG with the penetration of wind farms. The considered model is solved using a four-stage methodology and metaheuristic solvers. In [12], a multi-stage optimization framework was developed for optimal scheduling of flexible loads in a MG. The problem is formulated as a Mixed Integer Linear Programming (MILP) and seeks the worst-case scenario, determining if it can be satisfied by means of onsite generators and thus maximizing the efficiency of the system. Gholami, et al, developed in [13] a two-stage resilient-oriented scheduling program for MGs encompassing batteries and electric vehicles. In that reference, linearized approaches are used to convert the original nonlinear problem into a MILP.

Liu, et al [14] used robust optimization models for optimal scheduling a grid-connected MG, considering abrupt disconnection. To this end, the EMS ensures the self-supply capability by means of onsite generators, providing sufficient spinning reserves anytime according to forecast renewable generation. The method described in [15] considers correlation in PV generation and domestic consumption using Point Estimate methods (PEMs). The developed uncertainty modelling is incorporated into a nonlinear constrained scheduling model, which aims to minimize the total daily generation cost. In [16], a robust methodology is proposed for optimal scheduling of an energy intensive microgrid with wind and PV-based generators. In that reference, to avoid the high computational cost derived from robust formulation, the model is transformed to MILP by including a set of constraints.

Liu, et al presented in [17] a chance-constrained methodology for optimal scheduling of a grid-connected MG with BES and various kinds of renewable and non-renewable generators. The proposed solution procedure incorporates a scenario generation-reduction module combining stochastic and robust optimization procedures. Similarly, the model developed in [18] presents a min-max multi-objective function that considers operational cost and robustness on a whole. To that end, stochastic programming is used for uncertainties modelling, while the optimization procedure seeks for the worst-case scenario in which the scheduling result achieves the desired robustness. The authors in [19] developed a stochastic-based optimal scheduling/reconfiguration model for a MG with electric vehicles. In that formulation, curtailable loads are considered, whose expected demand can be partially non-satisfied on the basis of price-based DR initiatives.

The ref. [20] discusses the optimal bidding strategy for a MG aggregator. In the mathematical model, responsive loads provide flexibility to the operator to participate in energy markets. To determine the optimal bidding strategy of the aggregator, a robust optimization model was constructed, which considers unfavourable scenarios for renewable generation. In [21], the authors developed a tri-level recursive model for the optimal scheduling of MGs encompassing batteries. In that methodology, here-and-now and wait-and-see variables are jointly optimized, thus finding the worst-case realization of variables. Thereby, day-ahead scheduling obtained from wait-and-see variables is immune against uncertainties. A MG scheduling approach with consideration of utility grid failures and prevailing uncertainties was proposed in [22]. The developed mathematical model is formulated as a two-stage solution procedure by which the MG is scheduled for the worst-case realization of uncertainties.

Lee and Tuegeh [23] developed an optimal scheduling model for a grid-connected MG encompassing batteries and renewable generators. In that model, uncertainties from demand and renewable generation are considered and the optimization problem is solved using metaheuristic techniques. Likewise, the authors in [24] used a bio-inspired algorithm for solving the energy management problem of a grid-connected MG with BES, renewable generators, fuel-cell and microturbines, in which the uncertainties are treated via scenarios. In [25] a distributed energy management algorithm was developed for multi-MGs networks which consider uncertainties from demand, generation and also abrupt communication interruptions. The problem was formulated as a min-max objective that is solved using the Column-and-constraint generation algorithm to convert the original nonconvex problem into a solvable MILP. The authors in [26] investigated the optimal scheduling of an isolated multi-energy MG, encompassing electric, hydrogen and thermal subsystems. This model uses robust optimization to cope with uncertainties from demand and generation.

Dini, et al [27] proposed a hybrid stochastic-robust optimization approach for improving economic, reliability and security indicators of a grid-connected MG. The resulting nonlinear problem is converted into a MILP by employing different linearization techniques. In [28], a multi-time scale scheduling model is proposed for a MG encompassing BES. The developed formulation has scheduling capability for day-ahead and intraday horizons. Robustness against uncertainties is ensured by including spinning reserve constraints. A robust resilience-oriented MG scheduling model is presented in [29]. The developed formulation is second order and includes uncertainties from market price, renewable generation, demand and islanded event. During a disconnection event, the model contemplates the possibility of shedding load as a part of DR programs. Chen, et al developed in [30] a scheduling model for a rural MG encompassing energy storage. The developed methodology considers the Wassertein distance to uncertainties modelling and incorporates incentive-based DR consumers.

A MILP scheduling model for a domestic MG with consideration of users' satisfaction was developed in [31]. In that reference, a multi-objective approach is posed to jointly consider economic and comfort indexes that may be disrupted by deferring the operation of a set of flexible-loads. A second-order programming formulation for MG scheduling was proposed in [32], which incorporates frequency constraints to ensure the stability of the grid. In [33], a risk-averse model is developed for the energy management of a MG with PHS. The developed optimization procedure incorporates price-based DR programs based on time-of-use tariffs.

1.3 - Contributions & paper organization

As mentioned, this paper is focused on uncertainties modelling for MG scheduling. Specifically, this work is devoted to networks that encompass hybrid storage systems formed by BES and PHS. In this field, various research gaps have been detected based on the review above:

- Some formulations pose nonlinear constraints or objective functions that force to use of specific solvers or metaheuristic methodologies. However, MILP-based solution procedures are normally preferred because of its modular structure and global-optimum reachability [34].
- Stochastic programming is frequently used for uncertainty modelling. This approach leads to an expensive solution procedure due to all the variables are multidimensional, having the equal size to the number of scenarios generated.

Moreover, this approach needs a priori knowledge about the probability functions of uncertain parameters. Other references, however, proposed robust or interval optimization, which normally requires complex formulations or multi-stage procedures, that could provoke intractability issues as well.

- Most of the studied references only consider one storage technology (normally BES). This assumption does not allow to consider the effect of combining various storage technologies like batteries and PHS, thus hindering its analysis.
- Lastly, most of the references consider simple DR initiatives or simply neglect this kind of program. This simplification limits the scope of some works and nullifies the advantages of future smart grid paradigms in which consumers may partake actively.

This work is focused on filling the gaps above. To this end, this paper develops a novel interval-based formulation for optimal scheduling of MGs considering BES, PHS and DR programs. The new proposal is suitable for grid-connected MGs, thus including the volatility of energy pricing. As seen in Table 1, the present work overcomes the limitations of other related references. For the sake of simplicity, the main contributions and novelties of this article are numerated below:

- Developing a novel interval-based formulation for optimal scheduling of grid-connected MGs. This model accounts for uncertainty from renewable generation, demand and energy pricing, thus including a wide variety of uncertainties. The different parameters involved present a heterogeneous character, thus demonstrating the capability of the new proposal to handle naturally different uncertainties. The developed formulation takes advantage of confident intervals of the forecasted profiles to calculate an uncertainty-aware scheduling result, by which the impact of uncertainties is minimized. In contrast to other interval-based methodologies, the new proposal does not require the use of interval arithmetic, thus avoiding complex formulations and reducing the size of the problem. Thanks to the characteristics above, the developed model may find wide application in industry tools.

- In contrast to other references that present complex nonlinear models and metaheuristic-based solvers, the developed model is a MILP, which is modular and tractable by conventional solvers. This kind of formulation can be efficiently addressed by off-the-shelf solvers, being so tailorable to conventional software and finding multiple applications. On the other hand, the developed formulation is modular, being so adaptable to different scenarios and grid layouts.
- The developed model encompasses tractable but accurate yet models of BES and PHS, enabling the proper analysis of this hybrid storage facility.
- The impact of DR programs is analysed. To this end, price-based DR programs are properly modelled and included in the optimization procedure. Thus, its impact and role in hybrid storage systems for MGs can be analysed. This comprehensive model allows to properly analyse the interaction among these different agents and the possible advantages of DR and PHS in combination with conventional BES. This is profusely addressed by analysing different case studies with results.
- The effectiveness and efficiency of the new proposal are highlighted by comparing it with the Monte-Carlo simulation (MCS) which can be considered a benchmark for the uncertainties modelling approach [35].

Table 1 - Summary of the literature review

Ref.	Model	Uncertainties	BES	PHS	DR
[11]	Metaheuristic	Stochastic	Yes	No	No
[12]	MILP	Stochastic	No	No	Flexible loads
[13]	MILP	Stochastic	Yes	No	No
[14]	MILP	Robust	Yes	No	No
[15]	Nonlinear	PEM	No	No	No
[16]	MILP	Min-max	No	No	Flexible loads
[17]	MILP	Stochastic-Robust	Yes	No	No
[18]	MILP	Min-max	Yes	No	No
[19]	Nonlinear	Stochastic	Yes	No	Price-based
[20]	MILP	Robust	Yes	No	Price-based
[21]	Nonlinear	Robust	Yes	No	No
[22]	MILP	Min-max	Yes	No	No
[23]	Metaheuristic	Stochastic	Yes	No	No
[24]	Metaheuristic	Stochastic	Yes	No	No
[25]	MILP (iterative)	Min-max	Yes	No	Flexible-loads
[26]	MILP	Robust	Yes	No	Flexible-loads
[27]	MILP	Stochastic-Robust	Yes	No	Flexible-loads
[28]	Metaheuristic	No	Yes	No	Flexible-loads
[29]	Nonlinear	Robust	Yes	No	Sheddable-loads
[30]	MILP	Stochastic	Yes	No	Incentive-based
[31]	MILP	Stochastic	Yes	No	Flexible-loads
[32]	Nonlinear	Robust	Yes	No	No
[33]	Metaheuristic	Stochastic	No	Yes	Price-based
Present	MILP	Interval-based	Yes	Yes	Price-based

The new proposal is validated in three cases including, the deterministic model without price-based demand response (PBDR), the deterministic model with PBDR and interval-based model with PBDR. The simulation results verify the effectiveness of the interval-based formulation for the optimal scheduling of MGs with pumped-hydro and battery energy storage considering PBDR under uncertainty.

The rest of the paper is organized as follows: Section 2 presents the MG under study and the mathematical formulation. Uncertainty modelling using interval-based optimization is developed in Section 3. Section 4 describes case studies and presents various numerical simulations. This paper is concluded with Section 5.

2 - Mathematical modelling

Fig. 1 shows a typical grid-connected MG consisting of several energy producers and storage systems. In this section, the day-ahead scheduling of the mentioned MG considering the PBDR model is presented. The optimization problem is formulated as a Mixed Integer Non-Linear Programming problem that minimizes total cost. The big M technique is used to linearize the model and convert it into a MILP (see [36] for details). In this case, it is assumed that most local participants in the MG are geographically close to each other and more likely connected to the same distribution feeder. Based on this assumption, the power flow constraints of the distribution networks are not considered in the proposed model. This is a quite reasonable assumption in small-scale distribution feeders, where the power flow constraints are irrelevant [37]. In the following, the model of different equipment and optimization problem are developed.

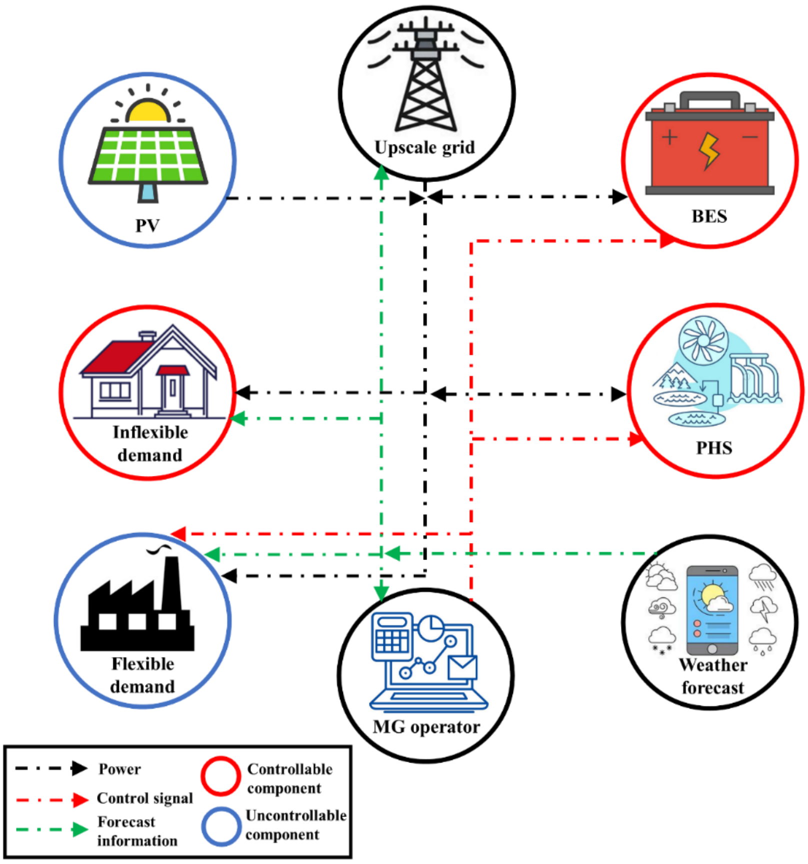

Figure - 1 Pictorial view of the MG under study

It is worth noting that this work is mainly focused on uncertainty modelling. In this regard, the operation in islanded mode has not been considered. This is due to the model would not be notably different in the case of being disconnected from the main grid. In such a case, the MG should probably account for a backup generator (maybe diesel generators) whose operation is totally deterministic. In this sense, some uncertainties related to energy pricing will not be modelled and therefore the contributions of the paper would be deteriorated. In this regard, we consider that the grid-connected mode is more suitable for uncertainties modelling since thus the uncertainties related to the energy pricing can be properly modelled and analyzed.

2.1 - PV panels model

The maximum power of a PV system depends on weather parameters, especially the amount of radiation and temperature [38]. In this work, assuming the availability of weather parameters, the production potential of the PV system is calculated as follows [39]:

$$p_t^{\mathrm{PV}} = \overline{p}^{\mathrm{PV}} \cdot [0.25 \cdot \vartheta_t + 0.03 \cdot \vartheta_t \cdot \theta_t + (1.01 - 1.13 \cdot \eta^{\mathrm{PV}}) \cdot (\vartheta_t)^2];\ \forall t \in \mathcal{T} \qquad (1)$$

However, as pointed out in [38], the eq. (1) does not consider the maximum power that can be extracted from the PV panels. Hence, the instantaneous power given by the PV system is limited by:

$$\underline{p}^{\mathrm{PV}} \leq p_t^{\mathrm{PV}} \leq \overline{p}^{\mathrm{PV}};\ \forall t \in T \qquad (2)$$

2.2 - Upscale grid model

The studied MG can purchase or sell energy from/to an upscale grid, which is assumed to be owned by a local utility. According to the power market contract, purchasing or selling energy for the MG is limited by (3). Moreover, the MG can only be energy purchaser or seller as forced by (4).

$$0 \leq p_t^{\mathrm{G.i}} \leq u_t^{\mathrm{G},i} \cdot \overline{p}^{\mathrm{G}};\ \forall \wedge t \in \mathcal{T} \wedge i \in \{\mathrm{buy}, \mathrm{sell}\} \qquad (3)$$

$$\sum_{\forall i \in \{\text{Buy,Sell}\}} \{u_t^{\text{G},i}\} \leq 1;\ \forall t \in \mathcal{T} \tag{4}$$

2.3 - BES model

The maximum power that can flow to/from batteries is limited by (5), which depends on the installed capacity and the energy-to-power ratio [40]. In addition, charging and discharging processes are complementary as forced by (6). Equation (7) models the batteries' state of charge while equation (8) limits the energy stored in the BES by the nominal capacity. In this work, it is assumed that the initial and final state of charge must be equal to maximum capacity as given in (9).

$$0 \leq p_t^{\text{BES},i} \leq u_t^{\text{BES},i} \cdot \frac{\overline{\varepsilon}^{\text{BES}}}{\text{e2P}};\ \forall \wedge t \in \mathcal{T} \wedge i \in \{\text{ch}, \text{dch}\} \tag{5}$$

$$\sum_{\forall i \in \{\text{ch,dch}\}} \{u_t^{\text{BES},i}\} \leq 1;\ \forall t \in \mathcal{T} \tag{6}$$

$$\varepsilon_t^{\text{BES}} = \varepsilon_{t-1}^{\text{BES}} + \Delta\tau \left(p_t^{\text{BES,ch}} \cdot \eta^{\text{BES}} - \frac{p_t^{\text{BES,dch}}}{\eta^{\text{BES}}} \right);\ \forall t \in \mathcal{T} \tag{7}$$

$$\underline{\varepsilon}^{\text{BES}} \leq \varepsilon_t^{\text{BES}} \leq \overline{\varepsilon}^{\text{BES}};\ \forall t \in \mathcal{T} \tag{8}$$

$$\varepsilon_{t=1}^{\text{BES}} = \varepsilon_{t=\text{size}(\mathcal{T})}^{\text{BES}} = \overline{\varepsilon}^{\text{BES}} \tag{9}$$

2.4 - PHS Model

The power exchanged between the PHS and the system depends on the flow range of water between upper and lower storage, proportional to the gravity acceleration, net head and water density, as modelled by (10) and (11) for the pumping and turbine processes, respectively [41]. Moreover, the flow range of water has been limited by (12).

$$p_t^{\text{PHS,t}} = \frac{g \cdot H \cdot \rho \cdot q_t^{\text{PHS,t}} \cdot \eta^{\text{PHS}}}{1000};\ \forall t \in \mathcal{T} \tag{10}$$

$$p_t^{\text{PHS,p}} = \frac{g \cdot H \cdot \rho \cdot q_t^{\text{PHS,p}}}{1000 \cdot \eta^{\text{PHS}}};\ \forall t \in \mathcal{T} \tag{11}$$

$$u_t^{\text{PHS},i} \cdot \underline{q}^{\text{PHS}} \leq q_t^{\text{PHS},i} \leq u_t^{\text{PHS},i} \cdot \overline{q}^{\text{PHS}};\ \forall t \in \mathcal{T} \wedge i \in \{\text{p}, \text{t}\} \tag{12}$$

Similar to the BES, the PHS system cannot work in the pump and turbine mode at the same time, which is ensured by imposing (13). On the other hand, (14) reflects coherency among the binary variables associated with the PHS operation.

$$\sum_{\forall i\in\{\mathrm{p,t}\}}\left\{u_t^{\mathrm{PHS},i}\right\} \leq 1;\ \forall t \in \mathcal{T} \tag{13}$$

$$\mathrm{on}_t^{\mathrm{PHS},i} - \mathrm{off}_t^{\mathrm{PHS},i} = u_t^{\mathrm{PHS},i} - u_{t-1}^{\mathrm{PHS},i};\ \forall t \in \mathcal{T}\backslash t > 1 \wedge i \in \{\mathrm{p,t}\} \tag{14}$$

The instantaneous water volume stored in the upper and lower reservoir is modelled by (15) and (16), respectively. In addition, the water volume stored in both reservoirs has to be limited by their capacity and a minimum required volume, as presented in (17).

$$v_t^{\mathrm{Upper}} = v_{t-1}^{\mathrm{Upper}} + 3600 \cdot \Delta\tau\left(q_t^{\mathrm{PHS,p}} - q_t^{\mathrm{PHS,t}}\right);\ \forall t \in \mathcal{T}\backslash t > 1 \tag{15}$$

$$v_t^{\mathrm{Lower}} = v_{t-1}^{\mathrm{Lower}} + 3600 \cdot \Delta\tau\left(q_t^{\mathrm{PHS,t}} - q_t^{\mathrm{PHS,p}}\right);\ \forall t \in \mathcal{T}\backslash t > 1 \tag{16}$$

$$\underline{v}^{\mathrm{PHS}} \leq v_t^i \leq \overline{v}^{\mathrm{PHS}};\ \forall t \in \mathcal{T} \wedge i \in \{\mathrm{Upper, Lower}\} \tag{17}$$

Similar to the BES, the initial and final energy stored in the PHS have been forced to be equal, which is established by (18) and (19). Finally, the ramping constraint for PHS is written by (20).

$$v_{t=1}^{\mathrm{Upper}} = v_{t=\mathrm{size}(\mathcal{T})}^{\mathrm{Upper}} = \overline{v}^{\mathrm{PHS}}; \tag{18}$$

$$v_{t=1}^{\mathrm{Lower}} = v_{t=\mathrm{size}(\mathcal{T})}^{\mathrm{Lower}} = \underline{v}^{\mathrm{PHS}}; \tag{19}$$

$$p_{t-1}^{\mathrm{PHS},i} - R^{\mathrm{PHS}} \leq p_t^{\mathrm{PHS},i} \leq p_{t-1}^{\mathrm{PHS},i} + R^{\mathrm{PHS}};\ \forall t \in \mathcal{T}\backslash t > 1 \wedge i \in \{\mathrm{p,t}\} \tag{20}$$

2.5 - MG power balance

To establish a coherent model, power balance must be preserved at any time (generation = demand). For the modelled MG, the power balance in MG at any time step is described by the following equation:

$$p_t^{\mathrm{G,buy}} + p_t^{\mathrm{PV}} + p_t^{\mathrm{B,dch}} + p_t^{\mathrm{PHS,t}} = p_t^{\mathrm{G,sell}} + D_t + p_t^{\mathrm{B,ch}} + p_t^{\mathrm{PHS,p}};\ \forall t \in \mathcal{T} \tag{21}$$

2.6 - PBDR Model

Since there are a variety of storage systems in the studied MG, a stepwise approximation-based PBDR scheme which is proposed in [42] is used in this paper. Five price levels are assumed here. The expected demand after applying PBDR can be given as:

$$D_t^{\mathrm{PBDR}} = D_t \cdot \sum_{j=1}^{j=J} u_t^{\mathrm{PBDR},j} \cdot L_j;\ \forall t \in \mathcal{T} \wedge j \in J \tag{22}$$

Equation (22) guarantees that only one price level can be active in each step time. Moreover, customer demand cannot be negatively impacted by the PBDR as forced by equation (24).

$$\sum_{\forall j \in \{J\}} \left\{ u_t^{\mathrm{PBDR},j} \right\};\ \forall t \in \mathcal{T} \tag{23}$$

$$\sum_{\forall t \in \{\mathcal{T}\}} \left\{ \sum_{\forall j \in \{J\}} \left\{ D_t \cdot u_t^{\mathrm{PBDR},j} \cdot L_j \right\} \right\} \geq \sum_{\forall t \in \{\mathcal{T}\}} \{D_t\};\tag{24}$$

2.7 - Objective function

In this work, the optimization problem consists of three parts as described in (25). The first part is the cost of energy exchanged with the upscale grid. The operation and maintenance costs of the PHS, BES and PV system are placed in the second part. Finally, the start-up and shut down cost of PHS are included in the third part.

To complete the optimization problem, the constraints that model the different MG components have to be considered. Therefore, the optimization model is completed by subjecting the objective function (25) to the constraints (1) - (24). It is worth noting that quadratic costs in (25) are linearized using piecewise representations (see [43] for details).

$$min\,F(x) = \sum_{\forall t \in \{\mathcal{T}\}} \left\{ \Delta\tau \left\{ \underbrace{\pi_t\left(p_t^{\text{G.buy}} - p_t^{\text{G.sell}}\right)}_{\substack{Electrical\ energy\ exchanged \\ with\ the\ upscale\ grid}} + \right. \right.$$

$$\left. \underbrace{\begin{matrix} \sum_{\forall i \in \{\text{pump,turb}\}}\{\mu^{\text{PHS}} \cdot p_t^{\text{PHS},i}\} \\ +\mu^{\text{BES}} \cdot \sum_{\forall i \in \{\text{ch,dch}\}}\left\{\left(p_t^{\text{BES},i}\right)^2\right\} + \mu^{PV} \cdot p_t^{PV} \end{matrix}}_{Operation\ and\ maintenance\ costs} \right\} +$$

$$\left. \underbrace{\sum_{\forall i \in \{\text{pump,turb}\}}\{\sigma^{\text{PHS}}\left(\text{on}_t^{\text{PHS},i} + \text{off}_t^{\text{PHS},i}\right)\}}_{Start-up\ and\ Shutdown\ costs} \right\} \tag{25}$$

3 - Developed interval-based formulation for uncertainties modelling

Since the behavior of the energy price in the deregulated power system is more dynamic than the vertical power market, the energy price uncertainty is modelled in this paper. In addition to the energy price, the uncertainties of the output power of the PV system and the load demand are also considered here. In this paper, an interval-based optimization is employed to account for the uncertainty of demand, energy price and PV output power. Due to the MILP structure, the developed interval-based approach can be easily adapted to different MG layouts encompassing a variety of energy resources. An optimization problem taking into account the uncertainties using the interval-based model can be written as follows [44]:

$$min\ \ F(x) \tag{26}$$

Subject to:

$$f_n(x) \le 0;\ \forall n \in N \tag{27}$$

$$g_k(x) \le [\underline{b}_k, \overline{b}_k];\ \forall k \in K \tag{28}$$

$$h_m(x) = [\underline{d}_m, \overline{d}_m];\ \forall m \in M \tag{29}$$

where x is decision variables and (26)-(29) denotes the objective function, deterministic constraints, interval-based inequalities constraint, and interval-based equalities constraint, respectively. In this work, (1), (3)-(20) and (22)-(24) are deterministic constraints, (21) and (25) are interval-based equalities, and (2) is interval-based inequality constraint, respectively. In addition, $[\underline{b}_k, \overline{b}_k]$ denotes interval variables of $[\underline{p_t^{\mathrm{PV,LB}}}, \underline{p_t^{\mathrm{PV,UB}}}]$ and $[\overline{p_t^{\mathrm{PV,LB}}}, \overline{p_t^{\mathrm{PV,UB}}}]$. $[\underline{d}_m, \overline{d}_m]$ indicates the interval forms of $\left[D_t^{PBDR,LB}, D_t^{PBDR,UB}\right]$ and $[\pi_t^{LB}, \pi_t^{UB}]$. The equality equations (21) and (25) can be replaced by (30) and (31), respectively.

$$p_t^{\mathrm{G.buy}} + p_t^{\mathrm{PV}} + p_t^{\mathrm{B,dch}} + p_t^{\mathrm{PHS,t}} = p_t^{\mathrm{G.sell}} + [D_t^{PBDR,LB}, D_t^{PBDR,UB}] + p_t^{\mathrm{B,ch}} + p_t^{\mathrm{PHS,p}};\ \forall t \in \mathcal{T} \tag{30}$$

$$min\, F(x) = \sum_{\forall t \in \{\mathcal{T}\}} \left\{ \Delta\tau \left\{ \underbrace{[\pi_t^{LB}, \pi_t^{UB}]\left(p_t^{\mathrm{G.buy}} - p_t^{\mathrm{G.sell}}\right)}_{\substack{Electrical\ energy\ exchanged \\ with\ the\ upscale\ grid}} + \underbrace{\begin{matrix} \sum_{\forall i \in \{\mathrm{pump,turb}\}} \left\{\mu^{\mathrm{PHS}} \cdot p_t^{\mathrm{PHS},i}\right\} + \\ \mu^{\mathrm{BES}} \cdot \sum_{\forall i \in \{\mathrm{ch,dch}\}} \left\{\left(p_t^{\mathrm{BES},i}\right)^2\right\} + \mu^{PV} \cdot p_t^{PV} \end{matrix}}_{operation\ and\ maintenance\ costs} \right\} + \underbrace{\sum_{\forall i \in \{\mathrm{pump,turb}\}} \left\{\sigma^{\mathrm{PHS}}\left(\mathrm{on}_t^{\mathrm{PHS},i} + \mathrm{off}_t^{\mathrm{PHS},i}\right)\right\}}_{Start-up\ and\ Shutdown\ costs} \right\} \tag{31}$$

And the inequality constraint can be rewritten as:

$$[\underline{p_t^{\mathrm{PV,LB}}}, \underline{p_t^{\mathrm{PV,UB}}}] \le p_t^{\mathrm{PV}} \le [\overline{p_t^{\mathrm{PV,LB}}}, \overline{p_t^{\mathrm{PV,UB}}}];\ \forall t \in \mathcal{T} \tag{32}$$

3.1 - Transformation and solution model

In the interval-based method, the probability degree is established to convert the interval-based equality and inequality constraints into deterministic ones. As a result, the problem will be solved utilizing the deterministic model. More details about the probability degree can be found in [44].

In the employed interval-based model, by considering the uncertainty as an interval of Z = $[\underline{z}, \overline{z}]$ and the real value of a, the probability degree is defined as follows:

$$P(a \leq b) = \begin{cases} 1, & a \leq \underline{z} \\ \frac{\overline{z}-a}{\overline{z}-\underline{z}}, & \underline{z} < a \leq \overline{z} \\ 0, & a > \overline{z} \end{cases} \tag{33}$$

In (33), it is assumed that the variable in the interval follows a uniform distribution, and P (a ≤ Z) indicates the probability degree for a ≤ Z. The value of the probability degree can vary depending on the level of risk considered by the operator where λ∈[0; 1]. When a ≤ Z, on the basis of (33), P (a ≤ Z) ≥ λ can be obtained as follows:

$$a \leq \underline{z}\lambda + \overline{z}(1 - \lambda) \tag{34}$$

According to the definition of probability degree, it is clear that λ is the level of risk that the operator considers to deal with uncertainties. If the operator chooses λ = 0 in equation (34), the interval-based inequality becomes to a ≤ $\overline{z}$, which is extremely optimistic and only the upper bound of the interval $[\underline{z}, \overline{z}]$ is considered. Also, if the operator chooses λ = 1, the interval-based inequality becomes to a ≤ $\underline{z}$, which is extremely pessimistic and tends to reduce the uncertainties of the interval $[\underline{z}, \overline{z}]$. As a result, the higher value of λ indicates the tighter bound of the uncertainties, or fewer risks that the operator considered and vice versa.

Based on the content of this section and using (34), the equation of interval-based model can be converted to deterministic ones as follows:

$$g_k(x) \le \underline{b}_k\lambda_{g,k} + \overline{b}_k(1-\lambda_{g,k});\ \forall k \in K \tag{35}$$

$$h_m(x) = \underline{d}_m\lambda_{h,m} + \overline{d}_m(1-\lambda_{h,m});\ \forall m \in M \tag{36}$$

So (30), (31) and (32) can be transformed to:

$$p_t^{\mathrm{G.buy}} + p_t^{\mathrm{PV}} + p_t^{\mathrm{B,dch}} + p_t^{\mathrm{PHS,t}} = p_t^{\mathrm{G.sell}} +$$

$$D_t^{PBDR,LB}\lambda_{h,m} + D_t^{PBDR,UB}(1-\lambda_{h,m}) + p_t^{\mathrm{B,ch}} + p_t^{\mathrm{PHS,p}};\ \forall t \in \mathcal{T} \tag{37}$$

$$min\, F(x) = \sum\nolimits_{\forall t\in\{\mathcal{T}\}} \left\{ \Delta\tau \left\{ \underbrace{(\pi_t^{LB}\lambda_{h,m} + \pi_t^{UB}(1-\lambda_{h,m}))\left(p_t^{\mathrm{G.buy}} - p_t^{\mathrm{G.sell}}\right)}_{\substack{Electrical\ energy\ exchanged \\ with\ the\ upscale\ grid}} + \right.\right.$$

$$\left. \underbrace{\begin{array}{c} \sum_{\forall i\in\{\mathrm{pump,turb}\}}\{\mu^{\mathrm{PHS}}\cdot p_t^{\mathrm{PHS},i}\} \\ +\mu^{\mathrm{BES}}\cdot\sum_{\forall i\in\{\mathrm{ch,dch}\}}\left\{\left(p_t^{\mathrm{BES},i}\right)^2\right\} + \mu^{PV}\cdot p_t^{PV} \end{array}}_{operation\ and\ maintenance\ costs} \right\} +$$

$$\left. \underbrace{\sum\nolimits_{\forall i\in\{\mathrm{pump,turb}\}}\left\{\sigma^{\mathrm{PHS}}\left(\mathrm{on}_t^{\mathrm{PHS},i} + \mathrm{off}_t^{\mathrm{PHS},i}\right)\right\}}_{Start-up\ and\ Shutdown\ costs} \right\} \tag{38}$$

$$\underline{p_t^{\mathrm{PV,LB}}}\lambda_{g,k} + \underline{p_t^{\mathrm{PV,UB}}}(1-\lambda_{g,k}) \le p_t^{\mathrm{PV}} \le \overline{p_t^{\mathrm{PV,LB}}}\lambda_{g,k} + \overline{p_t^{\mathrm{PV,UB}}}(1-\lambda_{g,k}) \quad ;\ \forall t \in \mathcal{T} \tag{39}$$

The step-by-step flowchart of implementing the proposed model is shown in Fig. 2

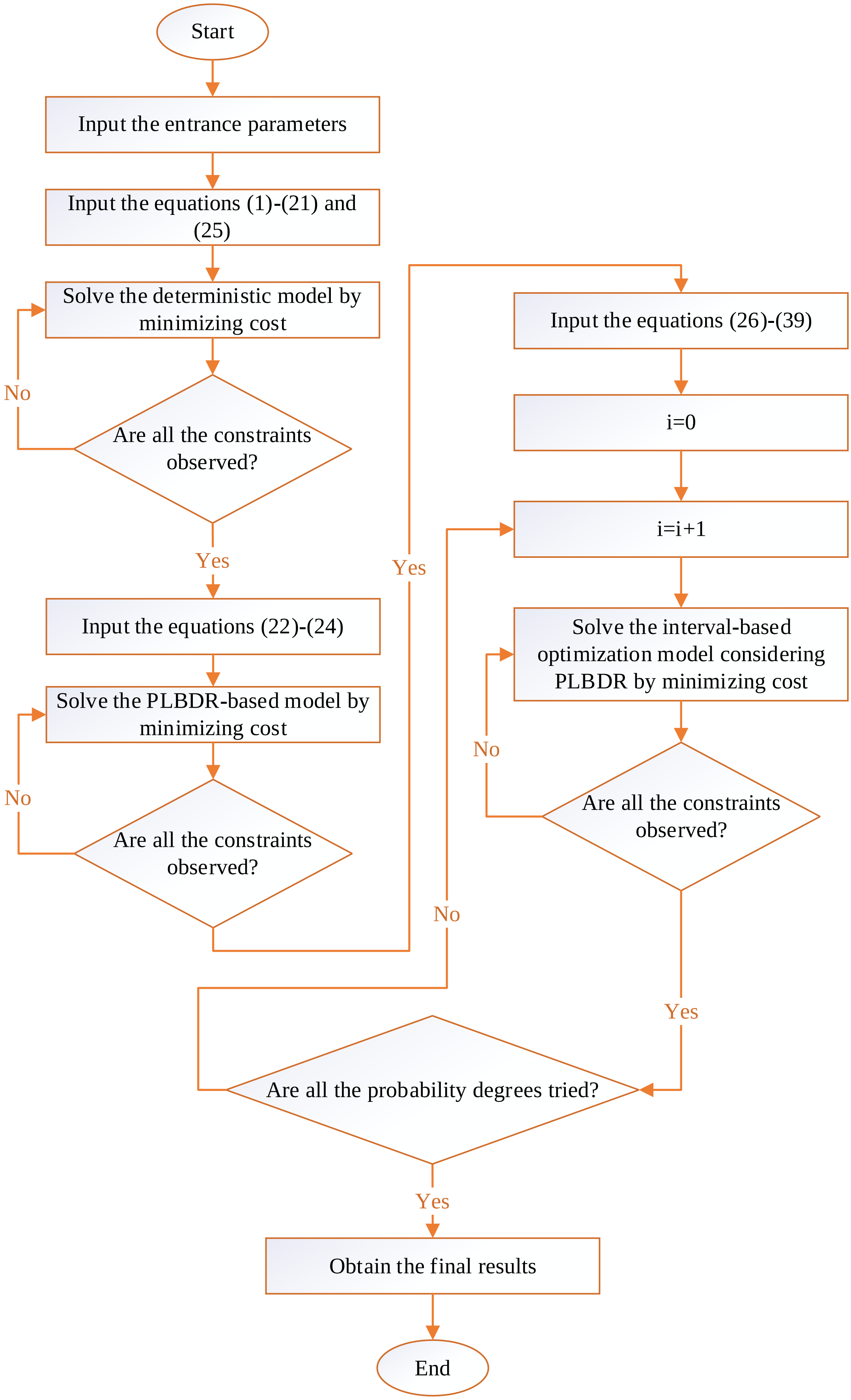

Figure 2 – the flowchart of proposed model

4 - Case study and numerical results

In this section, numerical results are carried out on the MG introduced in Section 2. The simulation is performed with two purposes: 1) analysing the effect of PBDR on the grid-connected MG; 2) investigating the impact of the interval-based optimization model considering electrical load, PV and energy price uncertainties. To cope with the mentioned purposes, the mathematical model proposed in sections 2 and 3 has been evaluated in three cases: 1) deterministic model without PBDR; 2) deterministic model with PBDR; 3) interval-based model with PBDR. The optimization problem has been conducted on an Intel® CoreTM i7, 12.00 GB RAM personal computer and solved over a 24 h time horizon with 15-min resolution. Table 2 shows the value of the parameters involved in simulations. Fig. 3 illustrates the forecast values of various weather parameters. These profiles were observed on May 3, 2016, at Virgin Islands (U.S.) [45]. Fig. 4 depicts the predicted local load at La Palma Island (Spain) on May 3, 2016 [46], and the hourly energy price at USA system NYISO on Dec 20, 2019 [47]. The purchase and sale prices of energy are considered equal to each other.

Table 2 - Input parameters

Parameter	Value	Parameter	Value
$\overline{D}/\underline{D}$	300/75 kW	$\overline{p}^{\mathrm{PV}}$	250 kW
$\overline{q}^{\mathrm{PHS}}/\underline{q}^{\mathrm{PHS}}$	2/0.1 m³/s	η^{PV}	0.167
$\eta^{\mathrm{PHS,p/t}}$	0.80	μ^{PV}	0.24 $/kWh
μ^{PHS}	0.31 $/kWh	$\overline{\varepsilon}^{\mathrm{BES}}$	100 kWh
$\overline{v}^{\mathrm{PHS}}/\underline{v}^{\mathrm{PHS}}$	6,000/500 m³	e2P	4 hrs.
R^{PHS}	150 kW	η^{BES}	0.95
σ^{PHS}	5 $	μ^{BES}	1×10^{-6} $/kWh²

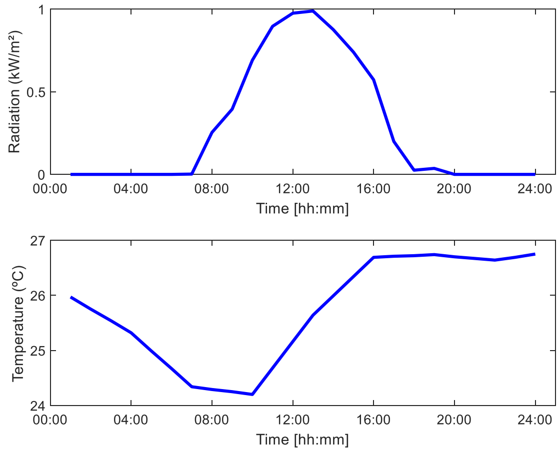

Figure 3 - The forecast values of various weather parameters (Solar radiation and Temperature)

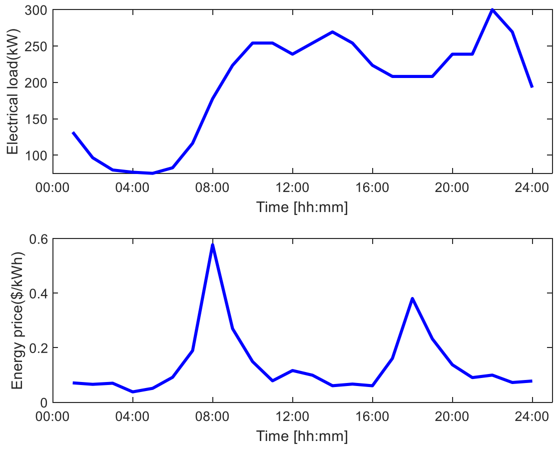

Figure 4 - The electrical load and energy exchanging price

4.1 - Deterministic model

Fig. 5 shows the power generated by PV that produces power close to the maximum power during peak hours. Interestingly, this correlation is related to a sunny day with the ideal temperature. Fig. 6 presents the energy exchanged between the MG and upscale grid considering (a) and without considering (b) storage systems. From the second subplot in Fig. 6 (a), it is apparent that the energy price has two peaks and the MG is the seller of energy in both peaks. As shown in Fig. 6 (b) the MG is the purchaser of energy at all times.

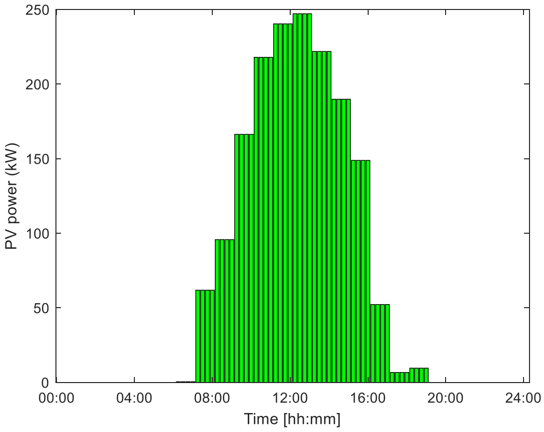

Figure 5 - The power generated by PV

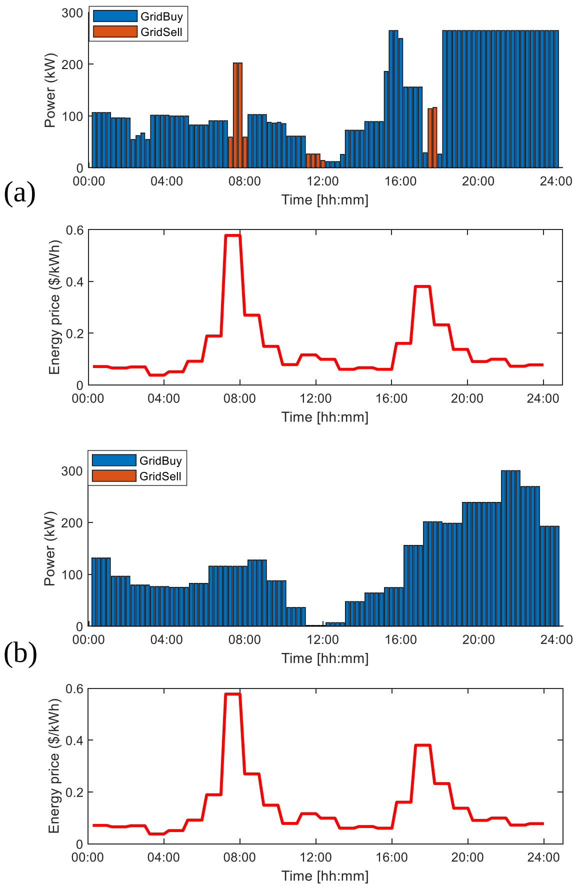

Figure 6 - Energy exchanged between MG and grid considering (a) and without considering (b) storage systems in the deterministic model

The volume of stored water in the upper and lower storage of PHS is shown in Fig. 7. Post hoc analysis revealed that during the peak of energy price, PHS operates in the turbine mode, and it operates in the pump mode during the off-peak of energy price.

Similar to PHS, the BES is in the discharging mode at the peak of the energy price and is being charged at the off-peak of the energy price as shown in Fig. 8.

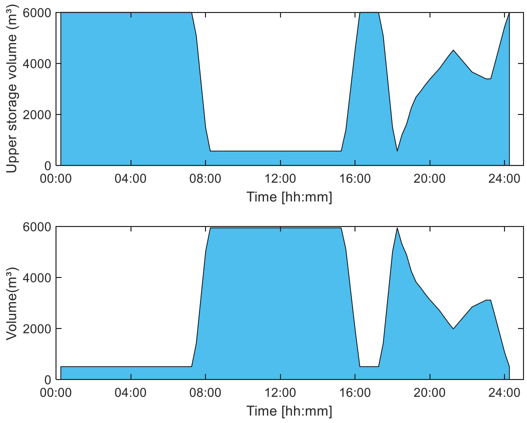

Fig. 7. Water volume stored in the upper (upper) and lower (bottom) reservoir of PHS in the deterministic model

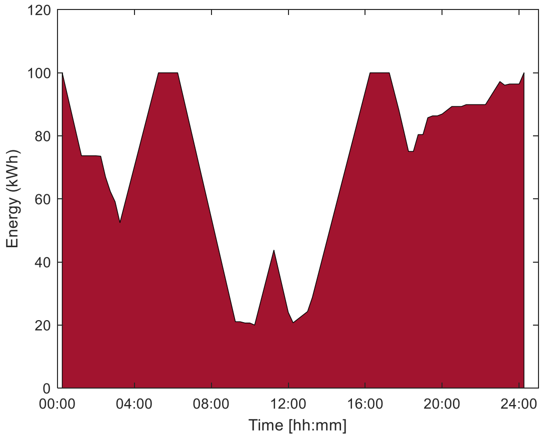

Figure 8 - Energy stored in the BES in the deterministic model

The balance of the power generation and the power consumption in the MG is presented in Fig. 9. It can be seen from this figure that the most of power generation is for responding to the electrical load which is propitiated by a high PV potential along with large PHS turbine generation. In this model, the total cost and total energy required to supply the electrical load are 415.23$ and 4671.4kWh, respectively.

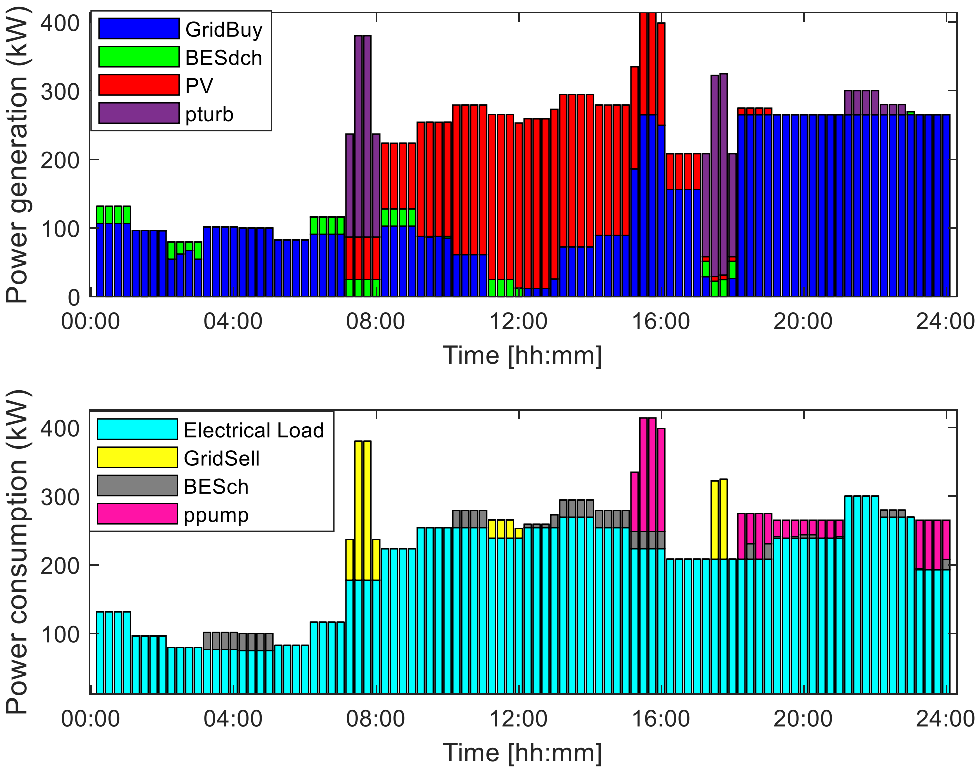

Fig. 9. The balance of the power generation and the power consumption in the MG in the deterministic model

4.2 - PBDR Model

There was a significant positive correlation between using PBDR and energy exchanging by the grid. As can be seen from Fig. 10, in the peaks of energy price and some other times, the MG sold energy to the grid. It has increased by 24% compared to the determinant model. What is interesting in this data is that the total energy exchanged between the MG and the grid has been increased by 4.41%, while the total energy required to supply the electrical load has not changed and is equal to 4672.7KWh. The most important reason for this event is that the MG has increased its energy purchases at the off-peak and its energy sales at the peak of energy price. It can be seen from Fig. 11, as energy prices rise, consumers are driven to reduce energy consumption, and as energy prices fall, consumers are driven to increase energy consumption. All of this has reduced the total cost by 15%.

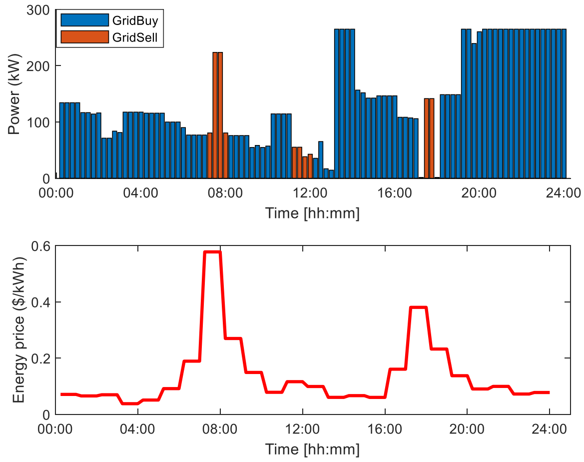

Figure 10 - Energy exchanged between MG and grid in the PBDR model

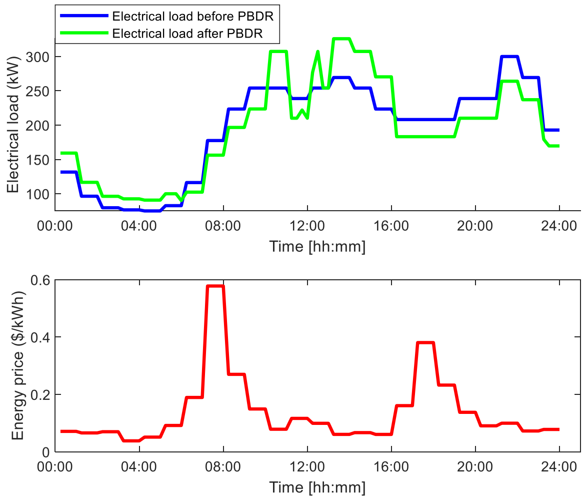

Figure 11 - The electrical load before and after PBDR compared to energy price

4.3 - Interval-based and PBDR model

In order to verify the proposed interval-based optimization problem, the model has been solved over a 24 h time horizon with 15 minutes resolution. The uncertainties of electrical load, PV generation and energy price have been considered. It should be noted that the uncertaintyy of energy prices is taken into account for the robustness of the model under-price variation. In this test simulation, we assume ±2.5% for the electrical load interval width, ±10% and ±5% error as the predicted values for the PV generation and energy price interval width respectively. In the simulation of λ_D, λ_{PV} and λ_{Pr} represent the probability degrees for uncertain intervals of the electrical load, PV generation and energy price, respectively. The optimization results under different conditions are listed in Table 3. The various cases are selected in such a way that both optimistic and pessimistic scenarios are considered for uncertain parameters.

Table 3 - The day-ahead total cost of the system for the interval-based and PBDR models

Cases	λ_D	λ_{PV}	λ_{Pr}	Cost ($)
1	0	1	0	358.72
2	0.5	1	0.5	333.25
3	1	1	1	313.16
4	1	0.5	1	311.86
5	1	0	1	310.55
6	0.7	0.6	0.5	328.29

As mentioned in section 4, choosing smaller values for λ_D and λ_{Pr} means larger values of electrical load and energy price respectively while choosing a larger λ_{PV} means smaller PV generation. As a result, case 1 represents the highest cost and Case 5 has the lowest cost as can be seen from Table II. It is notable that a higher energy price leads to an increase in the total cost because the MG is more the purchaser of energy.

Due to the high volume of results in this section, only the results related to case 6 are given. The allocated energy price and electrical load are shown in Fig. 12 and Fig. 13 respectively. It can be seen from Fig. 12 that the energy price is in the middle of an uncertain interval for the reason that the assigned probability degree of the energy price interval is equal to $\lambda_{Pr} = 0.5$. The electrical load is allocated close to the lower bound of uncertain interval because the assigned probability degree of the electrical load interval is high $(\lambda_D = 0.7)$. as shown in Fig. 14, the allocated PV power falls in the upper uncertain intervals which implies that the power generated by PV doesn't have any cost for the system. Furthermore, the allocated PV power is close to the lower bound of upper uncertain intervals as a result of $\lambda_{PV} = 0.6$.

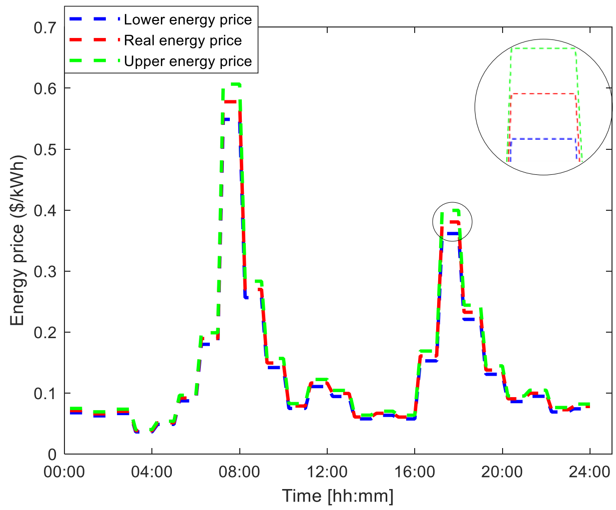

Figure 12 - The allocated energy price in the interval model

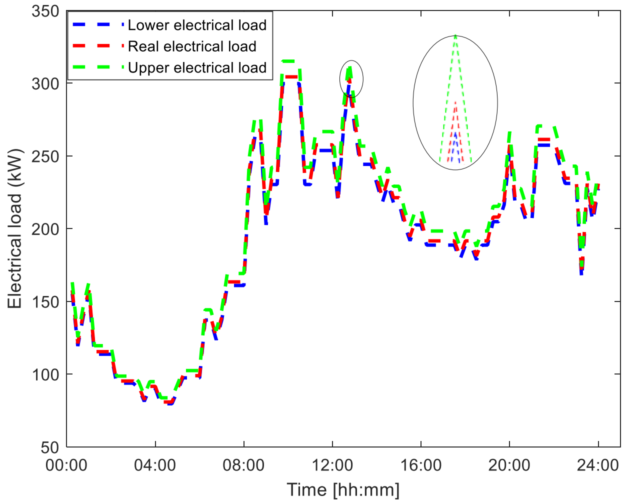

Figure 13 - The allocated electrical load in the interval model

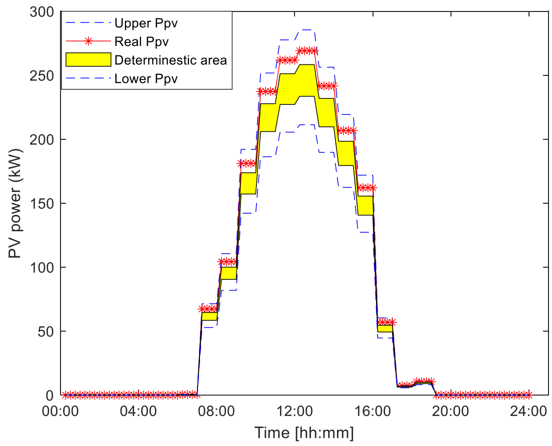

Figure 14 - The allocated PV power in the interval model

To compare the superiority of the proposed model over the conventional techniques, the problem is simulated using the MCS with similar conditions in case 6 [35]. According to the simulation results, the total cost with the MCS is 323.96$. the results show that the total cost with the MCS is close to the total cost with the proposed model, which is 328.29$. However, the total cost with the MCS is obtained with 3760 seconds, resulting in a high computational burden in comparison with the proposed model (57 seconds). This MCS run time is obtained with 100 stochastic scenarios. It is clear that for more stochastic scenarios, the simulation results are achieved in more computational time.

4.4 - Discussion

This section compares the results of the proposed models as can be seen from Table 4. The second column shows the total cost in different cases. As mentioned, in the PBDR model, the total cost has decreased significantly compared to the deterministic model. The total cost has also been reduced in the interval model because the electrical load is closer to the lower interval bound ($\lambda_D = 0.7$) and has a great impact on reducing the total cost. The third and fourth columns show the energy exchanged with the upscale grid which has the highest value in the PBDR model. The MG uses more storage systems because the electrical load is more flexible in this case. Increasing the use of storage systems rises the energy produced and consumed in the MG as shown in the fifth and sixth columns of Table 4.

Table 4 - Comparison of results obtained with various models

Cases	Total cost ($)	Total energy purchased from the grid (kWh)	Total energy sold to the grid (kWh)	Total energy generated in MG (kWh)	Total required energy (kWh)
Deterministic	415.23	3066.5	211.96	2315.9	5170.4
PBDR	353.04	3149	280.86	2326	5204
Interval and PBDR case 6	328.29	2837.6	19.51	1806.6	4624.7

5 - Conclusions and future works

A novel interval-based formulation for optimal scheduling of MGs considering BES, PHS and DR programs has been developed in this paper. The novel proposal is based on predicted confidence intervals of the forecasted profiles to produce an uncertainty-aware result by which the impact of uncertainties is minimized. A variety of uncertainties can be incorporated into the model as stated in this paper, in which the stochastic behavior of renewable generation, energy pricing and local demand have been managed

The developed methodology has been validated using various cases with aim of analysing the effect of PBDR and investigating the impact of the interval-based optimization model. The results show that the suggested approach can minimize the total operating cost and enhance the operational reliability of MG under the uncertainties.

In this regard, it has been shown that a notable cost reduction is achieved by enabling the PBDR (about 15%) while the total required energy of the system is increased. Moreover, the results have shown that the interval-based optimization has a significant influence on total operating cost (about 7% reduction in case 6) and the total required energy of the system (about 11% reduction in case 6). Besides, various cases of uncertainty showed that in an optimistic state the total cost can be reduced by 13.5% compared to the pessimistic state. Future works will be focused on applying similar formulations to other related problems under uncertain environments and also to planning tools.

References

[1] R. Sikkema, S. Proskurina, M. Banja, E. Vakkilainen. How can solid biomass contribute to the EU's renewable energy targets in 2020, 2030 and what are the GHG drivers and safeguards in energy- and forestry sectors?. *Renewable Energy* 2021; 165, Part I: 758-72. https://doi.org/10.1016/j.renene.2020.11.047.

[2] European Commission. Renewable Energy Directive I (2009/28/EC). 2009.

[3] European Commission. Renewable Energy Directive II (2018/2001/EC). 2018a.

[4] J. Yu, J. Yang, Y. Wu, D. Tang, J. Dai. Online state-of-health prediction of lithium-ion batteries with limited labeled data. *International Journal of Energy Research* 2020; 44(14): 11345-60. https://doi.org/10.1002/er.5750.

[5] F. Lin, J. Li, X. Hu, M. Sun. Study on the failure behavior of the current interrupt device of lithium-ion battery considering the effect of creep. *International Journal of Energy Research* 2020; 44(14): 11185-98. https://doi.org/10.1002/er.5689.

[6] H. Xu, M. Shen. The control of lithium-ion batteries and supercapacitors in hybrid energy storage systems for electric vehicles: A review. *International Journal of Energy Research* 2021; 45(15): 20524-44: https://doi.org/10.1002/er.7150.

[7] S. Bhol, N.C. Sahu. Decarbonizing the grid by optimal scheduling of solar PV-wind turbine-pumped hydro storage considering application on heuristic algorithms: A comprehensive review. *International Journal of Energy Research* 2021; 45(13): 18473-97: https://doi.org/10.1002/er.7036.

[8] S.A. Habeeb, et al. DC Nanogrids for Integration of Demand Response and Electric Vehicle Charging Infrastructures: Appraisal, Optimal Scheduling and Analysis. *Electronics* 2021; 10: 2484. https://doi.org/10.3390/electronics10202484.

[9] M. Tostado-Véliz, P. Arévalo, F. Jurado. A comprehensive electrical-gas-hydrogen Microgrid model for energy management applications. *Energy Conversion & Management* 2021; 228: 113726. https://doi.org/10.1016/j.enconman.2020.113726.

[10] P. Arévalo, M. Tostado-Véliz, F. Jurado. A novel methodology for comprehensive planning of battery storage systems. *Journal of Energy Storage* 2021; 37: 102456. https://doi.org/10.1016/j.est.2021.102456.

[11] B. Khorramdel, M. Raoofat. Optimal stochastic reactive power scheduling in a microgrid considering voltage droop scheme of DGs and uncertainty of wind farms. *Energy* 2012; 45(1): 994-1006. https://doi.org/10.1016/j.energy.2012.05.055.

[12] K. Liu, X. Guan, F. Gao, Q. Zhai, J. Wu. Self-balancing robust scheduling with flexible batch loads for energy intensive corporate microgrid. *Applied Energy* 2015; 159: 391-400. https://doi.org/10.1016/j.apenergy.2015.09.014.

[13] A. Gholami, T. Shekari, F. Aminifar, M. Shahidehpour. Microgrid Scheduling With Uncertainty: The Quest for Resilience. *IEEE Transactions on Smart Grid* 2016; 7(6): 2849-58. https://doi.org/10.1109/TSG.2016.2598802.

[14] G. Liu, M. Starke, B. Xiao, K. Tomsovic. Robust optimisation-based microgrid scheduling with islanding constraints. *IET Generation, Transmission & Distribution* 2017; 11(7): 1820-8. https://doi.org/10.1049/iet-gtd.2016.1699.

[15] S. Liu, P.X. Liu, X. Wang, Z. Wang, W. Meng. Effects of correlated photovoltaic power and load uncertainties on grid-connected microgrid day-ahead scheduling. *IET Generation, Transmission & Distribution* 2017; 11(14): 3620-7. https://doi.org/10.1049/iet-gtd.2017.0427.

[16] K. Liu, F. Gao. Scenario adjustable scheduling model with robust constraints for energy intensive corporate microgrid with wind power. *Renewable Energy* 2017; 113: 1-10. https://doi.org/10.1016/j.renene.2017.05.056.

[17] C. Liu, X. Wang, J. Guo, M. Huang, X. Wu. Chance-constrained scheduling model of grid-connected microgrid based on probabilistic and robust optimisation. *IET Generation, Transmission & Distribution* 2018; 12(11): 2499-509. https://doi.org/10.1049/iet-gtd.2017.1039.

[18] Y. Li, et al. Flexible Scheduling of Microgrid With Uncertainties Considering Expectation and Robustness. *IEEE Transactions on Industry Applications* 2018; 54(4): 3009-18. https://doi.org/10.1109/TIA.2017.2757902.

[19] M. Sedighizadeh, G. Shaghaghi-shahr, M. Esmaili, M.R. Aghamohammadi. Optimal distribution feeder reconfiguration and generation scheduling for microgrid day-ahead operation in the presence of electric vehicles considering uncertainties. *Journal of Energy Storage* 2019; 21: 58-71. https://doi.org/10.1016/j.est.2018.11.009.

[20] H. Khajeh, A.A. Foroud, H. Firoozi. Robust bidding strategies and scheduling of a price-maker microgrid aggregator participating in a pool-based electricity market. *IET Generation, Transmission & Distribution* 2019; 13(4): 468-77. https://doi.org/10.1049/iet-gtd.2018.5061.

[21] M.R. Ebrahimi, N. Amjady. Adaptive robust optimization framework for day-ahead microgrid scheduling. *International Journal of Electrical Power & Energy Systems* 2019; 107: 213-23. https://doi.org/10.1016/j.ijepes.2018.11.029.

[22] G. Liu, T. B. Ollis, Y. Zhang, T. Jiang, K. Tomsovic. Robust Microgrid Scheduling With Resiliency Considerations. *IEEE Access* 2020; 8: 153169-82. https://doi.org/10.1109/ACCESS.2020.3018071.

[23] C.-Y. Lee, M. Tuegeh. Optimal optimisation-based microgrid scheduling considering impacts of unexpected forecast errors due to the uncertainty of renewable generation and loads fluctuation. *IET Renewable Power Generation* 2020; 14(2): 321-31. https://doi.org/10.1049/iet-rpg.2019.0635.

[24] L. Luo, et al. Optimal scheduling of a renewable based microgrid considering photovoltaic system and battery energy storage under uncertainty. *Journal of Energy Storage* 2020; 28: 101306. https://doi.org/10.1016/j.est.2020.101306.

[25] H. Qiu, F. You. Decentralized-distributed robust electric power scheduling for multi-microgrid systems. *Applied Energy* 2020; 269: 115146. https://doi.org/10.1016/j.apenergy.2020.115146.

[26] S. Nojavan, A. Akbari-Dibavar, A. Farahmand-Zahed, K. Zare. Risk-constrained scheduling of a CHP-based microgrid including hydrogen energy storage using robust optimization approach. *International Journal of Hydrogen Energy* 2020; 45(56): 32269-84. https://doi.org/10.1016/j.ijhydene.2020.08.227.

[27] A. Dini, S. Pirouzi, M. Norouzi, M. Lehtonen. Hybrid stochastic/robust scheduling of the grid-connected microgrid based on the linear coordinated power management strategy. *Sustainable Grids & Networks* 2020; 24: 100400. https://doi.org/10.1016/j.segan.2020.100400.

[28] J. Zhang, et al. Multi-Time Scale Economic Scheduling Method Based on Day-Ahead Robust Optimization and Intraday MPC Rolling Optimization for Microgrid. *IEEE Access* 2021; 9: 140315-24. https://doi.org/10.1109/ACCESS.2021.3118716.

[29] N.M. Zografou-Barredo, et al. MicroGrid Resilience-Oriented Scheduling: A Robust MISOCP Model. *IEEE Transactions on Smart Grid* 2021; 12(3): 1867-79. https://doi.org/10.1109/TSG.2020.3039713.

[30] C.M. Chen, et al. Wasserstein distance-based distributionally robust optimal scheduling in rural microgrid considering the coordinated interaction among source-grid-load-storage. *Energy Reports* 2021; 7(3): 60-6. https://doi.org/10.1016/j.egyr.2021.05.073.

[31] H.P. Chen, L. Gao, Z. Zhang. Multi-objective optimal scheduling of a microgrid with uncertainties of renewable power generation considering user satisfaction. *International Journal of Electrical Power & Energy Systems* 2021; 131: 107412. https://doi.org/10.1016/j.ijepes.2021.107142.

[32] Z.D. Chu, N. Zhang, F. Teng. Frequency-Constrained Resilient Scheduling of Microgrid: A Distributionally Robust Approach. *IEEE Transactions on Smart Grid* 2021; 12(6): 4914-25. https://doi.org/10.1109/TSG.2021.3095363.

[33] Y. Zhao, J. Chen. A Quantitative Risk-Averse Model for Optimal Management of Multi-Source Standalone Microgrid with Demand Response and Pumped Hydro Storage. *Energies* 2021; 14: 2692. https://doi.org/10.3390/en14092692.

[34] N.G. Paterakis, O. Erdinç, A.G. Bakirtzis, J.P.S. Catalão. Optimal Household Appliances Scheduling Under Day-Ahead Pricing and Load-Shaping Demand Response Strategies. *IEEE Transactions on Industrial Informatics* 2015; 11(6): 1509-19. https://doi.org/10.1109/TII.2015.2438534.

[35] Mobasseri, Ali, Marcos Tostado-Véliz, Ali Asghar Ghadimi, Mohammad Reza Miveh, and Francisco Jurado. "Multi-energy microgrid optimal operation with integrated power to gas technology considering uncertainties." Journal of Cleaner Production 333 (2022): 130174. https://doi.org/10.1016/j.jclepro.2021.130174

[36] X. Kou, F. Li. Interval Optimization for Available Transfer Capability Evaluation Considering Wind Power Uncertainty. *IEEE Transactions on Sustainable Energy* 2020; 11(1): 250-9. https://doi.org/10.1109/TSTE.2018.2890125.

[37] C. Feng, F. Wen, S. You, Z. Li, F. Shahnia, M. Shahidehpour. Coalitional Game-Based Transactive Energy Management in Local Energy Communities. IEEE Transactions on Power Systems 2020; 35(3): 1729-1740. https://doi.org/10.1109/TPWRS.2019.2957537.

[38] M. Tostado-Véliz, S. Mouassa, F. Jurado. A MILP Framework for Electricity Tariff-choosing Decision Process in Smart Homes Considering 'Happy Hours' Tariffs. *International Journal of Electrical Power & Energy Systems* 2021; 131: 107139. https://doi.org/10.1016/j.ijepes.2021.107139.

[39] M. Tostado-Véliz, R. S. León-Japa, F. Jurado. Optimal electrification of off-grid smart homes considering flexible demand and vehicle-to-home capabilities. *Applied Energy* 2021; 298: 117184. https://doi.org/10.1016/j.apenergy.2021.117184.

[40] I. Alsaidan, A. Khodaei, W. Gao. A Comprehensive Battery Energy Storage Optimal Sizing Model for Microgrid Applications. *IEEE Transactions on Power Systems* 2018; 33(4): 3968-80. https://doi.org/10.1109/TPWRS.2017.2769639.

[41] A. Morabito, P. Hendrick. Pump as turbine applied to micro energy storage and smart water grids: A case study. *Applied Energy* 2019; 241: 567-79. https://doi.org/10.1016/j.apenergy.2019.03.018.

[42] B. Wang, C. Zhang, Z.Y. Dong. Interval Optimization Based Coordination of Demand Response and Battery Energy Storage System Considering SOC Management in a Microgrid.

IEEE Transactions on Sustainable Energy 2020; 11(4): 2922-31. https://doi.org/10.1109/TSTE.2020.2982205.
[43] M. Tostado-Véliz, P. Arévalo, F. Jurado. A comprehensive electrical-gas-hydrogen Microgrid model for energy management applications. *Energy Conversion & Management* 2021; 228: 113726. https://doi.org/10.1016/j.enconman.2020.113726.
[44] C. Huang, D. Yue, J. Xie, Y. Li, K. Wang. Economic dispatch of power systems with virtual power plant based interval optimization method. *CSEE Journal of Power and Energy Systems* 2016; 2(1): 74-80. https://doi.org/10.17775/CSEEJPES.2016.00011.
[45] National Centers for Environmental Information. Land-Based Datasets and Products. Online, available at: https://www.ncdc.noaa.gov/data-access/land-based-station-data/land-based-datasets, (accessed Dec. 16, 2021).
[46] REE. Canary electricity demand in real-time. Online, available at: https://www.ree.es/en/activities/canary-islands-electricity-system/canary-electricity-demand-in-real-time, (accessed Dec. 16, 2021).
[47] Y. Liu, C. Jiang, J. Shen, J. Hu. Coordination of Hydro Units With Wind Power Generation Using Interval Optimization. *IEEE Transactions on Sustainable Energy* 2015; 6(2): 443-53. https://doi.org/10.1109/TSTE.2014.2382122.